Gene Reports 37 (2024) 102036

Contents lists available at ScienceDirect

Gene Reports

journal homepage: www.elsevier.com/locate/genrep

Comparative genome composition of two closely related biocontrol strains of *Bacillus velezensis* endophytes

Kazeem A. Alayande, Ivan Schutte, Prudent Mokgokong, Rasheed Adeleke *

Unit for environmental Sciences and Management, North-West University, 11 Hoffman Street, Potchefstroom 2531, South Africa

ARTICLE INFO

Edited by Dominic Voon

Keywords:
Polyketides
Nonribosomal peptides
Renosterbos
Genome alignment
Point mutation

ABSTRACT

Comparative genomics was carried out between *Bacillus velezensis* KV10 and KV15 endophytes isolated from *Elytropappus rhinocerotis*. The nucleotides from the isolates were sequenced on an Illumina platform and assembled using SPAdes. Taxonomical identification was determined by a measure of evolutionary distance and codon-based phylogenetic trees. Sequence alignment against a representative isolate was assessed with Mauve, and a unique genomic region was determined through genome BLAST against a representative strain using GView. Protein family sorter and comparative pathway tools assigned to RASTtk4 were used to align the shared proteins between the isolates. antiSMASH was used to identify gene clusters for the bioactive secondary metabolites. Identification of mutant variants was determined through SNP calling using BWA-MEM to align the reads and FreeBayes for high-quality variants. *B. velezensis* KV10 and KV15 have genome sizes of 3,992,370 bp and 3,880,685 bp, and GC contents of 46.37 % and 46.49 %, respectively. There are identified genetic and evolutionary dissimilarities between the two endophytic isolates. Nineteen proteins with well-defined functions were found unique to KV10, while a total of thirty-two proteins were found unique to KV15. Missense or synonymous point mutations were observed at different loci in the KV10 genome; all affected codons are involved in the formation of polyketide synthase and general stress protein (*YdbA* and *YdbB*). The affected genes by point mutations in the KV15 are *YeeF* and *FliK*. Both strains contain gene clusters putative for biosynthesis of specific antimicrobial metabolites such as difficidin, macrolactin, fengycin, bacillibactin, bacillaene, and bacilysin. While only KV10 has additional gene clusters for mersacidin and surfactin biosynthesis. In addition, biosynthetic metabolites extracted from both strains exhibited notable antimicrobial effectiveness against test *Serratia marcescens* and *Fusarium* sp. Both isolates exhibit putative genetic features and are supported by in vitro assessment as promising candidates for biocontrol agents.

1. Introduction

There have been recent unwavering social campaigns and public concern about the extent of environmental degradation due to the age-long application of non-biodegradable agrochemicals on farmlands and post-harvest storage facilities. This potentially warrants intensified studies on developing more sustainable and eco-friendly biobased agrochemicals (Montso and Alayande, 2024). Biobased infection control in agricultural crops has a desirable potential for sustainable disease management practice, largely because it employs several competitive pathogen repression mechanisms such as direct antagonism, disruption of pathogen virulence determinants, induction of host-plant resistance, and sometimes degradation of pathogen activation signals (Subedi et al., 2020). Besides the aggressive and emerging consequences of changes in the climatic conditions, the large-scale losses of crops to pathogen attacks undermines global food security and threatens human survival (Lin et al., 2021). Bacterial strains with biocontrol capability often exhibit plant growth promotion traits, a value-added advantage that positions them as a consequential and valuable alternative to chemical-based synthetic pesticides in favour of much-anticipated green agricultural practices (Karthika et al., 2020).

Despite the great level of awareness of the resourcefulness of microorganisms of various kinds and tons of scientific studies addressing multi-facet challenges to salvage the deteriorating condition of global ecosystems, the 'green' resource has not been effectively tapped. A subset of this resource is the reservoir of endophytes hiding in between the tissues of diverse vegetation across all biomes. These endophytes are amazingly fortified with sophisticated molecular mechanisms for evolutionary adaptation; thus, represent important biological agents

* Corresponding author.
E-mail address: rasheed.adeleke@nwu.ac.za (R. Adeleke).

https://doi.org/10.1016/j.genrep.2024.102036
Received 7 June 2024; Received in revised form 30 August 2024; Accepted 14 September 2024
Available online 24 September 2024
2452-0144/© 2024 The Authors. Published by Elsevier Inc. This is an open access article under the CC BY-NC-ND license (http://creativecommons.org/licenses/by-nc-nd/4.0/).

Abbreviations

B. velezensis	*Bacillus velezensis*
GC	Guanine/Cytosine
DNA	Deoxyribonucleic acid
PBS	Phosphate Buffer Solution
BLAST	Basic Local Alignment Search Tool
SNP	Single-Nucleotide Polymorphism
NRP	Non-Ribosomal Peptides
PKS	Polyketide synthases
RiPP	Ribosomally synthesised and Post-translationally modified Peptides

that are playing an active role in plant defense mechanisms and as plant growth promotion indicators. Most endophyte strains share the same ecological niche with phytopathogens and secrete bioactive metabolites such as surfactins, Bacillibactin, macrolactin lipopeptides, mycobacillin etc. in defense of the host plants (Truyens et al., 2015; Morelli et al., 2020). Endophytes also put pathogens survival under check through synthesis of biochemicals such as siderophore, hydrogen cyanide, and activation of stress signaling hormones like jasmonate and ethylene (Tsipinana et al., 2023), therefore, they are considered more suitable as biocontrol agents.

Our current study is focused on the potential of developing biobased active agents against economically important crop pathogens from two closely related endophytic strains of *Bacillus velezensis* isolated from the leaves of *Elytropappus rhinocerotis*, commonly referred to as renosterbos. The plant is an important component of herbal medicine in the Cape region of South Africa and is being applied in folklore remedies against ailments such as diarrhoea, constipation, dyspepsia, peptic ulcers, cancer, cough, influenza, and skin infections (Hulley et al., 2019; Ndlovu et al., 2024). Bacillus species have demonstrated well-documented significant relevance in bioremediation, bioaugmentation, agricultural, and fermentation processes on an industrial scale. They are preferred in agricultural and industrial systems due to their ability to form spores that survive under heat exposure and desiccation and can be easily formulated into stable dry powder to improve their shelf-life (Rabbee et al., 2019). *Bacillus velezensis* is a novel species that is widely distributed in nature. It is non-virulent and non-pathogenic towards plants and animals. Several of its strains are enriched with pathways for the biosynthesis of secondary metabolites with broad-spectrum antimicrobials, stress tolerance and plant growth promotion mechanisms, and survival and stability strategies (Chen et al., 2019; Meng et al., 2016; Cui et al., 2020; Ye et al., 2018). Additionally, endophytic *B. velezensis* produces secondary metabolites that have the potential to trigger induced systemic resistance in the host plants, a phenomenon that activates the self-defense mechanisms of the host plant against recurrent attacks by virulent plant pathogens (Rabbee et al., 2019). The aim of this article is to adequately assess similarities and differences in the genetic composition and relevant putative functional capabilities of the two closely related biocontrol strains, *Bacillus velezensis* KV10 and *Bacillus velezensis* KV15 endophytes, isolated from *Elytropappus rhinocerotis*. The two strains were selected from among the best performing isolates as biocontrol agents.

2. Materials and methods

2.1. Collections of leaf samples and isolation of the endophytes

Leaves of *Elytropappus rhinocerotis* were harvested along the coastal region (S34° 27.811′ E20° 23.876′) of the Western Cape, South Africa. The leaf samples were surface sterilized successively in an 85 % ethanol and 3 % sodium hypochlorite solution and then rinsed with sterile distilled water. The effectiveness of the sterilization procedure was confirmed by plating a portion of the sterile leaves on nutrient agar and incubated at 37 °C for 24 h. The surface-sterilized leaves were carefully pulverized in liquid nitrogen to open up meristematic cells and other internal tissues before being cultured on tryptic soy agar and incubated at 37 °C for 48 h. Morphologically different bacterial colonies were isolated from the agar-culture plate and streaked out to obtain a pure culture for further studies.

2.2. Preliminary screening for biocontrol assessment

Isolated bacterial endophytes were cultured in Luria-Bertani (LB) broth for 72 h. The broth culture was centrifuged at 5000*g* for 5 min, and the supernatant was filtered through a 0.22 μm membrane filter. The susceptibilities of selected plant pathogens, *Serratia marcescens* and *Fusarium* sp., to the cell-free supernatant were determined using the agar well diffusion procedure as previously described (Alayande et al., 2017).

2.2.1. Determination of minimum inhibitory concentration (MIC)

The bioactive components in the cell-free metabolites were extracted into a mixture of chloroform and ethyl acetate (1:1 *v*/v) and thereafter lyophilized. The MIC of the crude active metabolites was determined using the agar dilution method. Two-fold dilutions of the freeze-dried metabolites were prepared in sterile distilled water to vary the concentration. Then 2 ml of each dilution factor was added to 18 ml of sterile molten MHA and PDA (Oxoid, UK) for the bacteria and fungi, respectively, to give final concentrations ranging from 0.16 to 5.0 mg/ml. The mixture was poured into sterile Petri dishes and allowed to set. Twenty-four hours old standard inoculums of the *S. marcescens* were streaked on each plate with different concentrations and incubated at 37 °C for 48 h. The spores of *Fusarium* sp. was harvested in 3 % glycerol and equally spread (100 μl) on PDA plates containing different concentrations of the bioactive metabolites, and thereafter incubated at 25 °C for 72 h. The plates were subsequently examined for the presence or absence of growth. The MIC was taken as the lowest concentration of the metabolite that inhibits growth of the pathogens. Sterile agar plates without the extract served as control.

2.3. Extraction and sequencing of the nucleotide materials

An 18 to 24 h old pure culture of the bacterial isolate in nutrient broth was centrifuged at 5000*g* for 5 min, and the cell pallets retrieved were washed three times in PBS under similar centrifugation conditions. DNA molecules were extracted from the washed cells using the Quick-DNA fungal/bacterial prep kit (Zymo Research, USA) following manufacturer instructions. The genomic DNA libraries were thereafter prepared with the Illumina Nextera DNA flex library prep kit before being sequenced on the Illumina MiSeq platform.

2.4. Preparation of the genome assembly and annotation

Total reads generated for *B. velezensis* KV10 were 12,367,076 while that of *B. velezensis* KV15 were 6,071,260, with 2 × 300-bp paired-end read lengths. The reads were filtered for low-quality fragments and adapter regions using Trimmomatic *v0.36* (Bolger et al., 2014) with a minimum quality score of 15 and a minimum sequence length of 70. The adapter sequences were clipped using a mismatch value of 2, a palindrome clip threshold of 30, and a simple clip threshold of 10. The assembly was performed with the sequenced reads using SPAdes *v3.15.3* (Bankevich et al., 2012; Prjibelski et al., 2020). The assembled genome was thereafter annotated using the NCBI Prokaryotic Genome Annotation Pipeline (PGAP) *v6.7* (Li et al., 2021) and Rapid Annotations using Subsystems Technology (RAST) with SEED viewer *v. 2.0* (Overbeek et al., 2014).

2.5. Taxonomic identification

Taxonomy assignments were obtained for both genomes using combination of the genome taxonomy database GTDB-Tk *v2.3.2* (Rodriguez-R et al., 2018), the genome blast distance phylogeny (GBDP), and amino acid/nucleotide-based phylogeny.

The GBDP tree was developed on the Type-strain genome server (TYGS) (Meier-Kolthoff and Göker, 2019). The genomes were compared against all type strain genomes available in the TYGS database via the MASH algorithm, a fast approximation of intergenomic relatedness (Ondov et al., 2016), to determine the closest type strains. The phylogeny was thereafter inferred through pairwise comparisons among the set of genomes and accurate intergenomic distances inferred under the algorithm 'trimming' and distance formula d_5. 100 distance replicates were calculated each. Digital DNA-DNA hybridization values and confidence intervals were calculated using the recommended settings of the GGDC 4.0 (Meier-Kolthoff et al., 2013,2022). The resulting intergenomic distances were used to infer a balanced minimum evolution tree with branch support through FASTME *v2.1.6.1*, including SPR postprocessing (Lefort et al., 2015). Branch support was inferred from 100 pseudo-bootstrap replicates, the tree rooted at the midpoint, and visualized with PhyD3 (Kreft et al., 2017).

The phylogeny was developed among 20 complete genomes of Bacillus species isolated from different sources in different parts of the world, as curated on the NCBI database. The comparison among the selected genomes hinged on a total of 500 randomly picked amino acid and nucleotide sequences from the BV-BRC global Protein Families (PGFams) (Davis et al., 2016). The alignment was built using MUSCLE (Edgar, 2004), and the nucleotide-coding gene sequences were aligned using the codon align function of BioPython (Cock et al., 2009). A concatenated alignment of all proteins and nucleotides was written to a PHYLIP-formatted file, and then a partitions file for RaxML *v8* (Stamatakis, 2014) was generated, describing the alignment in terms of the proteins and then the 1st, 2nd, and 3rd codon positions. Support values are generated using 100 rounds of the "Rapid" bootstrapping option of RaxML, and the resulting newick file was viewed using iTOL *v6* (Letunic and Bork, 2024).

2.6. Alignment and comparative genomics

The complete genome for each isolate was compared through nucleotide sequence alignment to identify different degrees of nucleotide rearrangements and possibly insertions and deletions using the progressiveMauve (Darling et al., 2010). Differences between the two genomes were further analyzed through genome BLAST against a representative genome (*Bacillus velezensis* JS25R) recovered from the NCBI database by comparing shared CDS, rRNA, and tRNA to determine unique genomic regions peculiar to each of the isolates under investigation using GView *v1.7* (Petkau et al., 2010). Additional comparative genomics was equally carried out using the protein family sorter and comparative pathway tools assigned to RASTtk4 through the BV-BRC annotation pipeline.

2.7. Single-nucleotide polymorphism genotyping

Genetic variations of single-nucleotide polymorphisms (SNPs) within the genome of each isolate were determined using BWA-MEM (Li, 2013) to align the reads for a read library, FreeBayes v1.3.6 (Marth et al., 1999) to generate high-quality variants for a read library, and snpEff v4.2 for prediction of the variant impact. All three pieces of software are hosted on the Bacterial and Viral Bioinformatics Resource Centre (BV-BRC) v3.36.16 platform (Olson et al., 2022).

2.8. In silico determination of bioactive metabolites

Rapid genome-wide in silico analysis of secondary metabolite biosynthesis gene clusters was assessed using antiSMASH v7.0 (Blin et al., 2023). We pre-set the software pipeline to only detect well-defined clusters containing all required parts of the nucleotide base putative for respective metabolites. The analysis included a combination of Known-Cluster-Blast for the identification of biosynthetic gene clusters from the MIBiG database and Sub-Cluster-Blast for the sub-cluster units. The conserved domain for RiPP recognition element (RRE) was determined by RRE-Finder to identify class-independent ribosomally-synthesised and post-translationally modified peptides (RiPP).

3. Results

3.1. Taxonomical identity

The two bacterial endophytes isolated from *Elytropappus rhinocerotis* were identified and assigned taxonomy as *Bacillus velezensis* KV10 and *Bacillus velezensis* KV15. The basic statistical features of the individual genome are summarized in Table 1. The identity of both isolates was further confirmed by inserting the genomes into a genome-scale distance tree and a codon tree based on shared encoding proteins. Drawing relatedness from the pairwise comparison and intergenomic distance among the type strains; and taking into consideration the similarities among species and subspecies clusters, GC contents, protein count, delta statistics, and genome size; *B. velezensis* KV10 showed a tightly close relationship with *B. velezensis* NRRL B-41580, a type strain isolated from Malaga city in Spain during the year 1999. *Bacillus velezensis* KV15 showed a close relationship with another type strain, *B. velezensis* KACC 13105, isolated from Cheongwon in South Korea during the year 2008 (Fig. 1). For the protein-based phylogeny, a total of 500 amino acids and nucleotides were explored to determine the level of relatedness among 20 selected *Bacillus* spp. from different regions across the globe. *Bacillus velezensis* KV10 formed a clade with a very strong bond (100 % bootstrap) with a representative strain, *B. velezensis* JS25R, isolated from China, while *B. velezensis KV15* also formed a tightly closed branch (100 % bootstrap) with the type strain, *B. velezensis* KACC 13105, isolated from South Korea (Fig. 2).

3.2. In vitro biocontrol assessment

The susceptibilities of *Serratia marcescens* and *Fusarium* sp. to the biosynthetic metabolites produced by the *Bacillus velezensis* strains were determined by measuring the apparent zones of inhibition. The zones of inhibition exhibited by *B. velezensis* KV10 against test *S. marcescens* and *Fusarium* sp. are 13.5 $\pm$ 0.5 and 19.6 $\pm$ 1.15 mm, respectively, while those of the KV15 are 20 $\pm$ 0.58 and 17 $\pm$ 1.53 mm, respectively. The minimum inhibitory concentrations exhibited by the metabolites extracted from KV10 are 1.25 and 2.5 mg/ml against *S. marcescens* and *Fusarium* sp., respectively, while that of KV15 was 1.25 mg/ml against both pathogens.

3.3. Comparative genomics

Conserved regions in the genomes of *B. velezensis* KV10 and KV15, and *B. velezensis* JS25R (a representative genome) were aligned by constructing positional homology multiple genome alignments (Fig. 3). When compared to the representative genome, there are three genome block inversions within the KV10 genome and one inversion in the KV15 strain. The inversion is shown by the upward or downward displacement on the horizontal alignment mapping, while the colour-coded blocks indicate shared genome fragments. On the other hand, genome BLAST of the two isolates against the representative genome conspicuously showed differences in unique genomic regions peculiar to each of the isolates (Fig. 4). In addition, annotation of the protein families for expression of differences and similarities between the two isolates and the representative strain is clustered into a heatmap for virtual observation and ease of comparison at a glance (Fig. 5). Besides hypothetical

Table 1
Statistical features of the genomes.

Isolates	Genome Size (bp)	Coverage	Contigs	N50	L50	GC (%)	CDS	Encoding proteins	Total RNAs	tRNAs
B. velezensis KV10	3,992,370	3×	10	2,015,708	1	46.37	3862	3801	63	58
B. velezensis KV15	3,880,685	2×	26	993,503	2	46.49	3903	3657	67	57

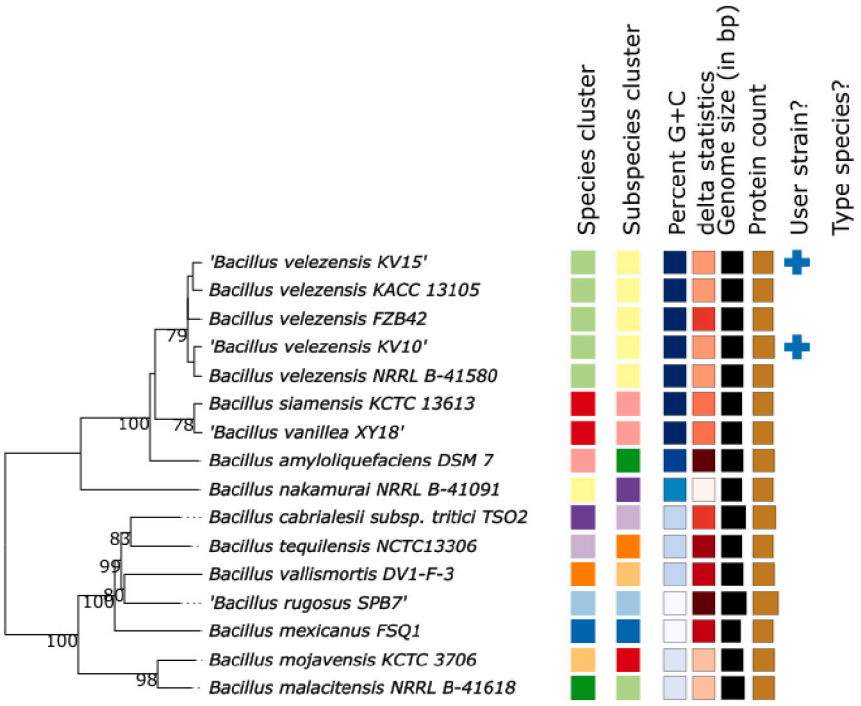

Fig. 1. Pairwise comparison and intergenomic distance phylogeny for the *B. velezensis* KV10 and *B. velezensis* KV15.

proteins, there are nineteen other well-defined proteins that are unique to *B. velezensis* KV10 (Table 2), and a total of thirty-two proteins are equally found only in *B. velezensis* KV15 (Table 3).

The single nucleotide polymorphism typing reveals 18 high-quality variants (Table 4) that have undergone single base-pair mutations, each at a specific locus in the genome of *B. velezensis* KV10. All the variants were affected by either missense or synonymous mutation with regards to the wildtype and have a low or moderate impact on the intrinsic features of the affected proteins. In the genome of *B. velezensis* KV15, only seven high-quality mutants were recovered, and all characterized as missense with moderate impact (Table 5).

3.4. Secondary metabolite gene clusters

Bacillus velezensis KV10 showed different gene clusters for the biosynthesis of eight different antimicrobial metabolites. The *B. velezensis* KV15 strain contains genetic information for six antimicrobial metabolites borne on different gene clusters. Both isolates shared the following classes of biosynthetic metabolites in common: polyketide (difficidin and macrolactin); non-ribosomal peptides, NRP (fengycin and bacillibactin); polyketide + NRP (bacillaene); and a dipeptide with nonproteinogenic L-anticapsin and N-terminal L-alanine (bacilysin), all at 100 % BLAST similarity (Fig. 6). Additional classes of biosynthetic metabolites found only in the *B. velezensis* KV10 strain are RiPP:Lanthipeptide (mersacidin) and NRP:Lipopeptide (surfactin), with 100 % and 82 % BLAST similarities respectively (Fig. 7).

4. Discussion

Endophytes are sustainable alternative producers of natural products and a promising resource for biocontrol agents. The complex metabolic interactions between endophytes and host plants have a pronounced influence on the diversity of biosynthetic active metabolites produced by both symbiotic partners, and the integrity of its pharmacological efficacy. Endophyte-derived bioactive metabolites could be an indispensable source for novel drug discoveries. Although the full potential is often limited by conventional laboratory cultivation, with the advent of omics technology and genetic engineering, a lot more can be deciphered (Zotchev, 2024). In this article, we compare the genomic components of two closely related strains of *Bacillus velezensis* endophytes that have demonstrated promising potential as good candidates for biocontrol agents.

During preliminary in vitro screening, both isolates demonstrated effective antimicrobial capabilities against *Serratia marcescens* and *Fusarium* sp. selected as plant pathogens. *Serratia marcescens* has been reportedly implicated in yellow vine disease in watermelon, pumpkin, and cucurbits (Sikora et al., 2012; Besler and Little, 2017), soft rot in red pepper (Gillis et al., 2014), whorl rot in maize (Wang et al., 2015), yellow wilt in sunflower (Ignatov et al., 2016), leaf rot in industrial hemp (Schappe et al., 2020), and black rot in orange fruits (Hasan et al., 2020). And on the other hand, major tropical fruits such as avocado, banana, mango, papaya and pineapple are equally susceptible to the infection caused by *Fusarium* species both while on the field and during postharvest storage, causing root, stem, and fruit rots and vascular wilt (Zakaria, 2023).

Taxonomical identification based on evolutionary distance and

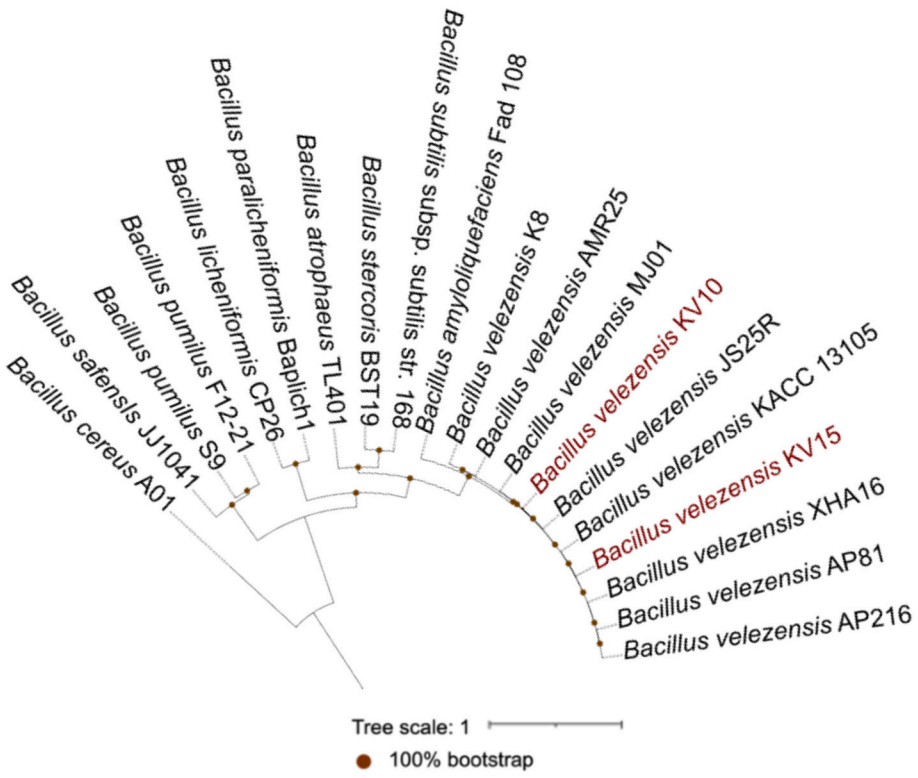

Fig. 2. Shared protein-based phylogeny for the *B. velezensis* KV10 and *B. velezensis* KV15.

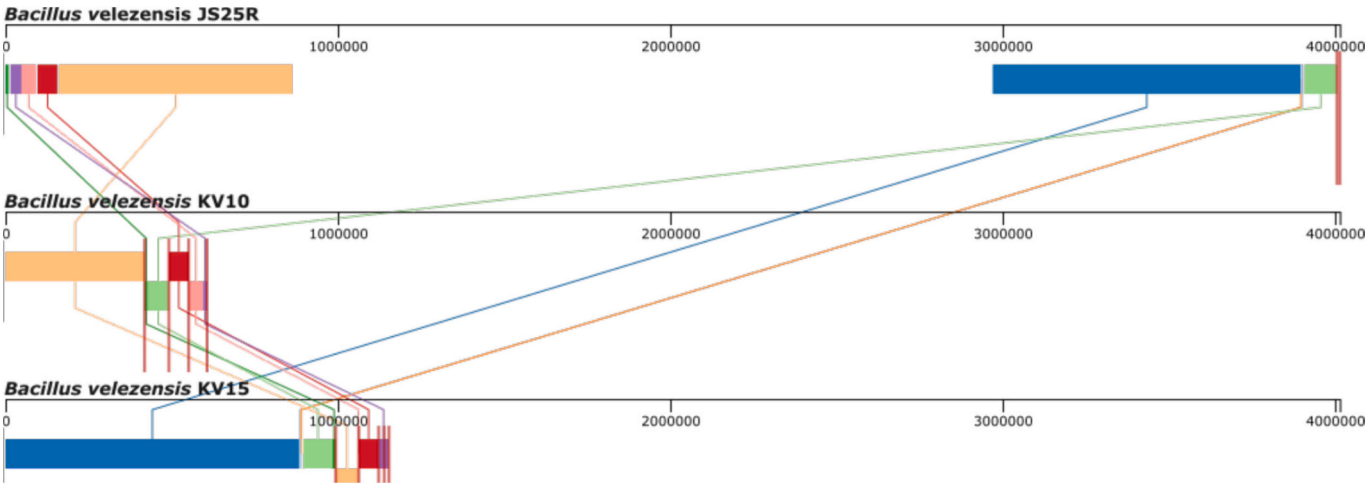

Fig. 3. Positional homology multiple genome alignments with progressiveMauve.

comparison among shared amino acids and nucleotides suggested preliminary differences in the genetic make-up of both isolates. *Bacillus velezensis* KV15 showed a repeated tightly close evolutionary relationship and proximity with *B. velezensis* KACC 13105 on two different forms of phylogenetic trees. It can be inferred that both strains shared a lot of genetic features. The strain KACC 13105 was isolated in 2008 from rice rhizosphere soil and KV15 was isolated in 2023 as an endophyte from *Elytropappus rhinocerotis*, a dominant plant in the Western cape region of South Africa. Alignment of the conserved regions and mapping of the unique genomic regions of *B. velezensis* KV10 and *B. velezensis* KV15 against the representative isolate, *B. velezensis* JS25R, further confirmed the level of differences and similarities between the two endophytic bacterial isolates. *B. velezensis* KV10 has three inverted genome blocks, while *B. velezensis* KV15 has only one of its genome blocks that underwent an inversion at a genome fragment dissimilar to that of *B. velezensis* KV10. Each of the isolates indicates distinct unique genomic regions after genome BLAST against a representative strain, as well as differences and similarities in the protein families that characterized their genetic compositions.

Moreover, among the protein families that are found unique only to *B. velezensis* KV10 are phage genome-assembly-supporting and infective-cycle timing proteins, which include Prophage Lp1 protein 19, Phage portal protein, Phage major capsid protein, Phage capsid and scaffold, Phage terminase large subunit, and Holin. And the only phage-related protein family found in *B. velezensis* KV15 is Prophage LambdaBa02, DNA replication protein. Moreso, tailed bacteriophages account for more than a thousand known virions; they use a limited number of structural arrangements to build stable infectious viral particles. For

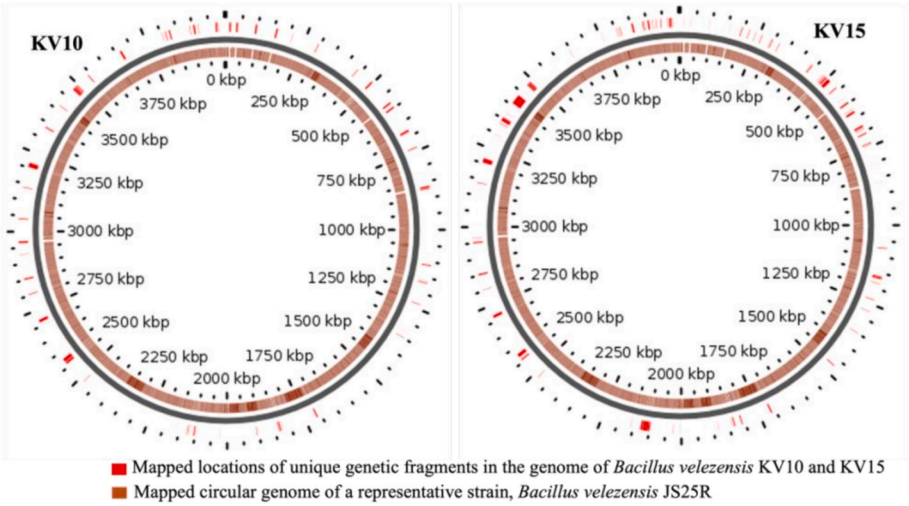

Fig. 4. Mapping of the genome blast for detecting unique regions peculiar to each isolate using GView *v1.7*.

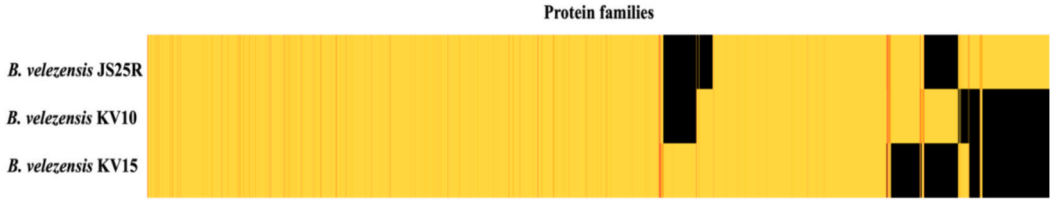

Fig. 5. The heatmap showing clustered protein families in both isolates as compared to a representative genome, the colour code indicates number of copies of a gene.

Table 2
List of well-defined proteins unique to *Bacillus velezensis* KV10.

Description of the proteins	Length of amino acids
Competence regulatory protein ComQ	291
Dimeric dUTPase (EC 3.6.1.23)	222
DNA-cytosine methyltransferase (EC 2.1.1.37)	336
HIT family hydrolase	110
Holin	140
Hydrolase, HAD superfamily	270
Myo-inositol 2-dehydrogenase (EC 1.1.1.18)	341
Phage capsid and scaffold	138
Phage major capsid protein	305
Phage portal protein	467
Phage terminase, large subunit	404
Prophage Lp1 protein 19	229
PTS system, beta-glucoside-specific IIA, IIB & IIC component	611
Restriction enzyme *BcgI* alpha chain-like protein (EC:2.1.1.72)	676
Sulfate and thiosulfate binding protein CysP	342
Sulfate and thiosulfate import ATP-binding protein CysA (EC 3.6.3.25)	356
Sulfate transport system permease protein CysT	278
Sulfate transport system permease protein CysW	287
Uncharacterized protein YybG	283

instance, scaffolding proteins steer phage assembly by chaperoning the major capsid protein in the tailed bacteriophage-herpesvirus lineage to assemble an icosahedral lattice that protects the linear dsDNA viral genome (Ignatiou et al., 2019). Also, holins are small proteins that accumulate in the cell membrane over a fixed period of time readily programmed into the holin gene, thus controlling the length of the infective cycle for lytic phages (Wang et al., 2000).

In addition, we equally observed genetic variation on specific loci separately in the genomes of *B. velezensis* KV10 and KV15 through SNP calling. Eighteen mutant variants were recovered from the strain KV10, none of which resulted in major functional changes. Sixteen of the affected codons are involved in the functionality of polyketide synthase and related proteins. Only one is involved in the general stress protein (*YdbA* and *YdbB*), and the remaining one contributes to the intergenic region. Polyketide synthases (PKSs) are remarkable multifunctional large molecular-size catalytic proteins. They are responsible for the biosynthesis of a structurally diverse range of bioactive secondary metabolites with significant broad-spectrum pharmacological potentials (Robbins et al., 2016). The presence of this protein family is evident in the high number of identified gene clusters putatively producing secondary metabolites in *B. velezensis* KV10. The fact that every locus affected by point mutation resulted in either missense or synonymous variation suggests that the ability of the isolate to produce multiple natural products with a broad spectrum remains intact and unaffected. Equally, among the seven identified point mutations in *B. velezensis* KV15, six of them occurred on the loci responsible for the *YeeF* gene, five of which are missense mutations and one synonymous with low to moderate impact. The *YeeF* gene encodes for polymorphic toxins that help in the growth arrest of competing neighbouring organisms, disruption of the operon that could disadvantage the possessing bacteria, driving selection of kins, and shaping the microbiome through spatial segregation of different bacterial strains (Kaundal et al., 2020; Kobayashi, 2021). It is again important to underscore the fact that the presence of the *YeeF* gene in *B. velezensis* KV15 equally suggests the strain as a good candidate for biocontrol agents.

Furthermore, both *B. velezensis* KV10 and KV15 contain multiple gene clusters for the biosynthesis of secondary metabolites of pharmacological importance. Difficidin and macrolactin are the two members of the polyketide group of bioactive metabolites found in common with both isolates. Polyketide synthases (PKS) are multi-modular enzymes that are involved in the biosynthesis of polyketide secondary metabolites in microorganisms. Polyketides are regarded as one of the richest classes of drug gold-mine; they are extremely diverse in structure and

Table 3
List of well-defined proteins unique to *Bacillus velezensis* KV15.

Description of the proteins	Length of amino acids
2,3-dihydro-2,3-dihydroxybenzoate dehydrogenase (EC 1.3.1.28) of siderophore biosynthesis	261
3-methylitaconate Delta isomerase (EC 5.3.3.6)	376
Carboxymuconolactone decarboxylase (EC 4.1.1.44)	138
Carboxymuconolactone decarboxylase (EC 4.1.1.44)	133
Carboxysome protein CcmM	214
Cell wall surface anchor family protein, LPXTG motif	184
Cinnamyl alcohol dehydrogenase/reductase (EC 1.1.1.195) @ Alcohol dehydrogenase (EC 1.1.1.1)	349
Enoyl-CoA hydratase (EC 4.2.1.17)/3-hydroxyacyl-CoA dehydrogenase (EC 1.1.1.35)/3-hydroxybutyryl-CoA epimerase (EC 5.1.2.3)	168
FIG. 045374: Type II restriction enzyme, methylase subunit YeeA	904
Lactoylglutathione lyase and related lyases	128
Late competence protein ComEA, DNA receptor	204
Lipopolysaccharide core biosynthesis protein RfaZ	109
Lipopolysaccharide core heptosyltransferase I	77
Lysine-arginine-ornithine-binding ABC transporter, substrate-binding protein ArgT (TC 3.A.1.3.1)	206
Mannose-6-phosphate isomerase	121
Membrane protein, distant similarity to thiosulphate:quinone oxidoreductase DoxD	129
Mobile element protein	162
N-acetyl-L,L-diaminopimelate aminotransferase homolog	389
Na+/H+ antiporter	523
Outermost layer of the spore maturation protein CgeB	318
Prophage LambdaBa02, DNA replication protein	169
Putative toxin component near putative ESAT-related proteins, repetitive	93
Ring-cleaving dioxygenase MhqE	307
Ring-cleaving dioxygenase MhqO	312
Rrf2 family transcriptional regulator	167
Spore coat polysaccharide biosynthesis protein SpsG; N-acylneuraminate cytidylyltransferase (EC 2.7.7.43)	334
Two-component transcriptional response regulator, LuxR family	78
Uncharacterized beta-barrel protein YwiB	142
Uncharacterized membrane protein YCR061W	59
Uncharacterized protein YybS	311
Uncharacterized UPF0750 membrane protein	209
UPF0702 transmembrane protein YdfR	194

Table 4
High quality variants detected in the genome of *B. velezensis* KV10.

Wildtype	Variants	Coverage	Functions	Types	Impact
ACG	ACA	10	Polyketide synthase and related proteins	Synonymous	Low
AAG	AAA	6	Polyketide synthase and related proteins	Synonymous	Low
GCG	GTA	7	Polyketide synthase and related proteins	Missense	Moderate
GAC	GAT	13	Polyketide synthase and related proteins	Synonymous	Low
ACG	ACA	16	Polyketide synthase and related proteins	Synonymous	Low
GGT	GGC	13	Polyketide synthase and related proteins	Synonymous	Low
CGC	CGT	14	Polyketide synthase and related proteins	Synonymous	Low
AAATTG	AAGCTG	14	Polyketide synthase and related proteins	Synonymous	Low
GAC	GAT	15	Polyketide synthase and related proteins	Synonymous	Low
GCC	ACC	18	Polyketide synthase and related proteins	Missense	Moderate
GACCCC	GATCCG	35	Polyketide synthase and related proteins	Synonymous	Low
TAC	TAT	35	Polyketide synthase and related proteins	Synonymous	Low
GGC	GAC	17	Polyketide synthase and related proteins	Missense	Moderate
AAA	AAC	19	Polyketide synthase and related proteins	Missense	Moderate
ATC	ATT	19	Polyketide synthase and related proteins	Synonymous	Low
GGA	AGC	16	Polyketide synthase and related proteins	Missense	Moderate
GNN	GCN	12	General stress protein (YdbA & YdbB)	Synonymous	Low
		15	tRNA-Gly-TCC	Intergenic region	Modifier

biological activities (Qadri, 2022). Polyketide difficidin produced by the endophytic *B. amyloliquefaciens* FZB42 was established to have significant antimicrobial activity against *Erwinia amylovora*, a bacterial pathogen responsible for fire blight disease in orchard trees (Chen et al., 2009). Similarly, difficidin produced by *B. amyloliquefaciens* WHI disrupted cell membrane integrity of *Ralstonia solanacearum*, a bacterial pathogen that causes widespread bacterial wilt disease in many plants (Liu et al., 2023). In another study, macrolactin J produced by *Bacillus* sp. ZJ318 also exhibited strong antibacterial activity (Zhang et al., 2022). In a similar vein, application of macrolactin R extracted from an endophytic *B. siamensis* YB304 substantially reduced the disease symptoms of *Botrytis cinerea* infected strawberries through cell membrane disruption, causing leakages of vital cellular components and eventual cell death (Ni et al., 2023).

Additionally, the biosynthesis of nonribosomal peptides (NRP) is another class of bioactive metabolites found on specific gene clusters in both KV10 and KV15 strains. NRPs are structurally diverse and have a wide range of pharmacological applications. Their natural diversity is due to a series of evolutionary processes over many years, including the accumulation of gene duplication, genetic recombination, and horizontal gene transfer (Zhang and Kries, 2023). The diversity is further enhanced by their susceptibility to modification through acylation, glycosylation, oxidation, and phosphorylation (Ranjan et al., 2023). NRPs have attracted several studies due to their valuable applications in medicine and agriculture. They are produced by multifunctional nonribosomal peptide synthetase enzymes that are of variable sizes and organised in modules composed of adenylation, thiolation, and condensation core domains (Duban et al., 2022). An example of nonribosomal peptides found in both isolates is fengycin, which is an important member of the lipopeptide family with a wide range of applications in agriculture and pharmaceutics. It induces resistance in

Table 5
High quality variants detected in the genome of *B. velezensis* KV15.

Wildtype	Variants	Coverage	Function	Types	Impact
CGC	GGG	163	*YeeF*	Missense	Moderate
GGA	AGA	172	*YeeF*	Missense	Moderate
GAT	GAA	179	*YeeF*	Missense	Moderate
ATT	ATC	174	*YeeF*	Synonymous	Low
CTCGAATTG	CTTGATCTG	158	*YeeF*	Missense	Moderate
GAA	GAT	174	*YeeF*	Missense	Moderate
NNC	NGC	116	Formerly; flagellar hook-length control protein FliK	Synonymous	Low

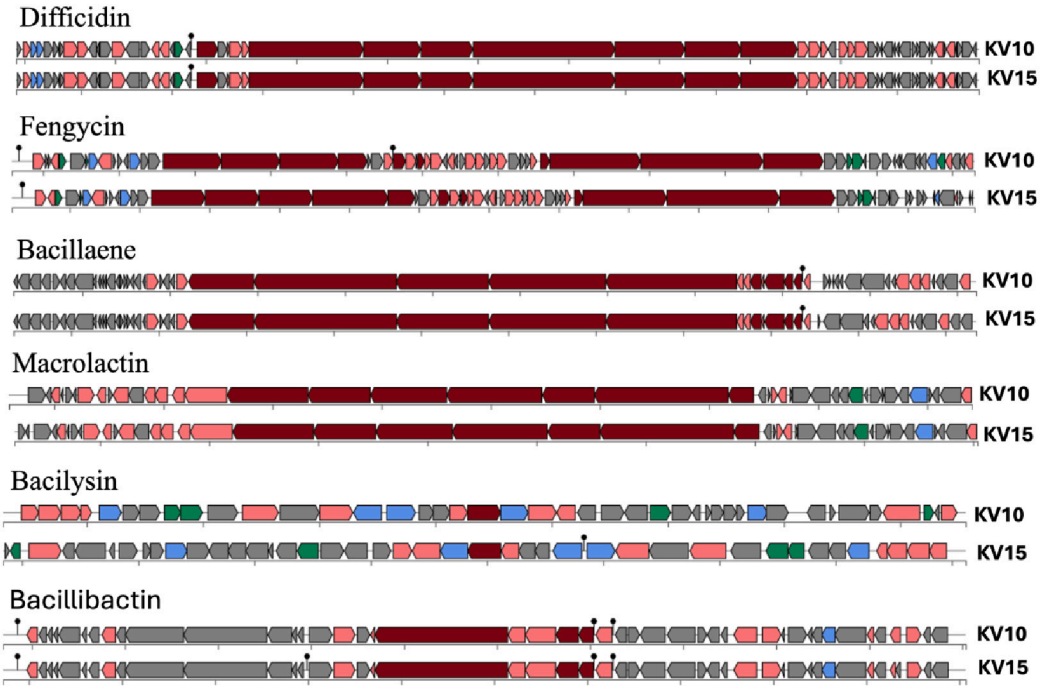

Fig. 6. Biosynthetic metabolites gene clusters (■) found common to both *B. velezensis* KV10 and *B. velezensis* KV 15; ⊥ Binding site.

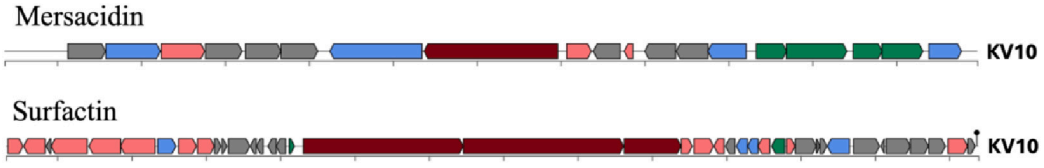

Fig. 7. Biosynthetic metabolites gene clusters (■) found only in the *B. velezensis* KV10; ⊥ Binding site.

plants and, as well, attacks the phospholipid bilayer in filamentous fungi, causing structural damage and thus disrupting the selective permeability of the cell membrane (Yin et al., 2024).

It is important to note that mersacidin and surfactin are other bioactive secondary metabolites with corresponding gene clusters only represented in *B. velezensis* KV10. Mersacidin is a class II lanthipeptide antimicrobial metabolite, a member of the ribosomally synthesised and post-translationally modified peptides (RiPPs). They are characterized by intramolecular lanthionine rings responsible for the structure and stability of their bioactive components (Viel and Kuipers, 2022). Their intramolecular structures are susceptible to bioengineering for novel natural products of pharmacological importance. Mersacidin employs obstruction of cell wall biosynthesis through effective inhibition of polymeric peptidoglycan as a mode of biocidal action (Brötz et al., 1995). On the other hand, surfactin is a cyclic lipopeptide and one of the most potent biosurfactants first identified from the culture medium of *B. subtilis*. Its structure is composed of an amino acid chain attached to a fatty acid chain. It is also known to possess a range of biological activities such as haemolysis, prevention of blood clotting, and antimicrobial efficacy (Rahman et al., 2021). Surfactin has good interfacial and functional properties coupled with moisturising and cleansing features and it is widely applied in the cosmetics, detergents, and food industries (Bueno-Mancebo et al., 2024). Surfactin is a broad-spectrum antimicrobial agent; it attacks pathogens through cell membrane disruption, prevention of protein synthesis, blockage of cell division, and obstruction of metabolic pathways through enzyme inhibition (Chen et al., 2022). The combination of all the identified putative bioactive metabolites found in both *B. velezensis* KV10 and KV15 broadly supports the need to further unearth more endophytic organisms as targets for novel biosynthetic agrochemicals and direct biocontrol agents for sustainable agriculture.

5. Conclusion

Despite *Bacillus velenzensis* KV10 and KV15 having several background factors in common, both isolates have specific differences in their genetic composition. This is more evident in the large numbers of hypothetical proteins and a few other proteins with defined features that were found unique to each isolate, as well as the single nucleotide polymorphisms (SNPs). Secondly, the significance of endophytes as resourceful organisms for the anticipated green agricultural and industrial revolutions cannot be overemphasized. Preliminary screening indicated that both isolates are effective in repressing the growth of the test plant pathogens. This capability is further supported by the genetic information found in both strains which are notable for biosynthesis of multiple bioactive metabolites of pharmacological importance. This positions each of them as a suitable candidate for a biocontrol agent and offers a great advantage for further exploration of these endophytes in search of novel natural products.

CRediT authorship contribution statement

Kazeem A. Alayande: Writing – review & editing, Writing – original draft, Visualization, Validation, Supervision, Software, Methodology, Investigation, Data curation. **Ivan Schutte:** Writing – review & editing, Validation, Methodology, Investigation. **Prudent Mokgokong:** Writing – review & editing, Visualization, Validation, Supervision. **Rasheed Adeleke:** Writing – review & editing, Visualization, Validation, Supervision, Resources, Project administration, Methodology, Investigation, Funding acquisition, Data curation, Conceptualization.

Declaration of competing interest

The authors declare that they have no known competing financial interests or personal relationships that could have appeared to influence the work reported in this paper.

Data availability

All data information has been provided in the manuscript

Acknowledgments

The authors acknowledge the National Research Foundation (NRF), South Africa, for the funding (grant unique number: USDB200420515055).

References

Alayande, K.A., Pohl, C.H., Ashafa, A.O.T., 2017. Time-kill kinetics and biocidal effect of *Euclea crispa* leaf extracts against microbial membrane. Asian Pac J Trop Med 10 (4), 390–399. https://doi.org/10.1016/j.apjtm.2017.03.022.

Bankevich, A., Nurk, S., Antipov, D., Gurevich, A.A., Dvorkin, M., Kulikov, A.S., Lesin, V. M., Nikolenko, S.I., Pham, S., Prjibelski, A.D., Pyshkin, A.V., Sirotkin, A.V., Vyahhi, N., Tesler, G., Alekseyev, M.A., Pevzner, P.A., 2012. SPAdes: a new genome assembly algorithm and its applications to single-cell sequencing. J. Comput. Biol. 19, 455–477.

Besler, K.R., Little, E.L., 2017. Diversity of Serratia marcescens strains associated with cucurbit yellow vine disease in Georgia. Plant Dis. 101 (1), 129–136.

Blin, Kai, Shaw, Simon, Augustijn, Hannah E., Reitz, Zachary L., Biermann, Friederike, Alanjary, Mohammad, Fetter, Artem, Terlouw, Barbara R., Metcalf, William W., Helfrich, Eric J.N., van Wezel, Gilles P., Medema, Marnix H., Weber, Tilmann, 2023. antiSMASH 7.0: new and improved predictions for detection, regulation, chemical structures, and visualization. Nucleic Acids Res. 46 (5), 702–716.

Bolger, A.M., Lohse, M., Usadel, B., 2014. Trimmomatic: a flexible trimmer for Illumina sequence data. Bioinformatics 30, 2114–2120.

Brötz, H., Bierbaum, G., Markus, A., Molitor, E., Sahl, H.G., 1995. Mode of action of the lantibiotic mersacidin: inhibition of peptidoglycan biosynthesis via a novel mechanism? Antimicrob. Agents Chemother. 39 (3), 714–719.

Bueno-Mancebo, J., Barrena, R., Artola, A., Gea, T., Altmajer-Vaz, D., 2024. Surfactin as an ingredient in cosmetic industry: benefits and trends. Int. J. Cosmet. Sci.

Chen, X.H., Scholz, R., Borriss, M., Junge, H., Mögel, G., Kunz, S., Borriss, R., 2009. Difficidin and bacilysin produced by plant-associated Bacillus amyloliquefaciens are efficient in controlling fire blight disease. J. Biotechnol. 140 (1–2), 38–44.

Chen, L., Shi, H., Heng, J., Wang, D., Bian, K., 2019. Antimicrobial, plant growth-promoting and genomic properties of the peanut endophyte Bacillus velezensis LDO2. Microbiol. Res. 218, 41–48.

Chen, X., Lu, Y., Shan, M., Zhao, H., Lu, Z., Lu, Y., 2022. A mini-review: mechanism of antimicrobial action and application of surfactin. World J. Microbiol. Biotechnol. 38 (8), 143.

Cock, P.J., Antao, T., Chang, J.T., Chapman, B.A., Cox, C.J., Dalke, A., Friedberg, I., Hamelryck, T., Kauff, F., Wilczynski, B., De Hoon, M.J., 2009. Biopython: freely available Python tools for computational molecular biology and bioinformatics. Bioinformatics 25 (11), 1422.

Cui, L., Yang, C., Wei, L., Li, T., Chen, X., 2020. Isolation and identification of an endophytic bacteria Bacillus velezensis 8-4 exhibiting biocontrol activity against potato scab. Biol. Control 141, 104156.

Darling, A.E., Mau, B., Perna, N.T., 2010. progressiveMauve: multiple genome alignment with gene gain, loss and rearrangement. PLoS One 5 (6), e11147.

Davis, J.J., Gerdes, S., Olsen, G.J., Olson, R., Pusch, G.D., Shukla, M., Vonstein, V., Wattam, A.R., Yoo, H., 2016. PATtyFams: protein families for the microbial genomes in the PATRIC database. Front. Microbiol. 7, 118.

Duban, M., Cociancich, S., Leclère, V., 2022. Nonribosomal peptide synthesis definitely working out of the rules. Microorganisms 10 (3), 577.

Edgar, R.C., 2004. MUSCLE: multiple sequence alignment with high accuracy and high throughput. Nucleic Acids Res. 32 (5), 1792–1797.

Gillis, A., Rodríguez, M., Santana, M.A., 2014. Serratia marcescens associated with bell pepper (Capsicum annuum L.) soft-rot disease under greenhouse conditions. Eur. J. Plant Pathol. 138, 1–8.

Hasan, M.F., Islam, M.A., Sikdar, B., 2020. First Report of *Serratia Marcescens* Associated With Black Rot of *Citrus Sinensis* Fruit, and Evaluation of its Biological Control Measures in Bangladesh. F1000Research, p. 9.

Hulley, I., Van Vuuren, S., Sadgrove, N., Van Wyk, B.-E., 2019. Antimicrobial activity of Elytropappus rhinocerotis (Asteraceae) against micro-organisms associated with foot odour and skin ailments. J. Ethnopharmacol. 228, 92–98.

Ignatiou, A., Brasilès, S., El Sadek Fadel, M., Bürger, J., Mielke, T., Topf, M., Tavares, P., Orlova, E.V., 2019. Structural transitions during the scaffolding-driven assembly of a viral capsid. Nat. Commun. 10 (1), 4840.

Ignatov, A.N., Khodykina, M.V., Polityko, V.A., Sukhacheva, M.V., 2016. First report of Serratia marcescens causing yellow wilt disease on sunflower in Russia. New Disease Reports 33 (8), 2044-0588.

Karthika, S., Varghese, S., Jisha, M., 2020. Exploring the efficacy of antagonistic rhizobacteria as native biocontrol agents against tomato plant diseases. 3 Biotech 10 (7), 320.

Kaundal, S., Deep, A., Kaur, G., Thakur, K.G., 2020. Molecular and biochemical characterization of YeeF/YezG, a polymorphic toxin-immunity protein pair from Bacillus subtilis. Front. Microbiol. 11, 512166.

Kobayashi, K., 2021. Diverse LXG toxin and antitoxin systems specifically mediate intraspecies competition in Bacillus subtilis biofilms. PLoS Genet. 17 (7), e1009682.

Kreft, L., Botzki, A., Coppens, F., Vandepoele, K., Van Bel, M., 2017. PhyD3: a phylogenetic tree viewer with extended phyloXML support for functional genomics data visualization. Bioinformatics 33, 2946–2947.

Lefort, V., Desper, R., Gascuel, O., 2015. FastME 2.0: a comprehensive, accurate, and fast distance-based phylogeny inference program. Mol. Biol. Evol. 32, 2798–2800.

Letunic, I., Bork, P., 2024. Interactive Tree of Life (iTOL) v6: recent updates to the phylogenetic tree display and annotation tool. Nucleic Acids Res. gkae268.

Li, H., 2013. Aligning sequence reads, clone sequences and assembly contigs with BWA-MEM. In: Computer Science, Biology arXiv: Genomics. https://doi.org/10.6084/M9.FIGSHARE.963153.V1.

Li, W., O'Neill, K.R., Haft, D.H., DiCuccio, M., Chetvernin, V., Badretdin, A., Coulouris, G., Chitsaz, F., Derbyshire, M.K., Durkin, A.S., Gonzales, N.R., 2021. RefSeq: expanding the prokaryotic genome annotation pipeline reach with protein family model curation. Nucleic Acids Res. 49 (D1), D1020–D1028.

Lin, L., Xu, K., Shen, D., Chou, S.H., Gomelsky, M., Qian, G., 2021. Antifungal weapons of Lysobacter, a mighty biocontrol agent. Environ. Microbiol. 23, 5704–5715.

Liu, N., Sun, H., Tang, Z., Zheng, Y., Qi, G., Zhao, X., 2023. Transcription factor Spo0A regulates the biosynthesis of Difficidin in Bacillus amyloliquefaciens. Microbiol. Spectrum 11 (4), e01044-23.

Marth, G.T., Korf, I., Yandell, M.D., Yeh, R.T., Gu, Z., Zakeri, H., Stitziel, N.O., Hillier, L., Kwok, P.Y., Gish, W.R., 1999. A general approach to single-nucleotide polymorphism discovery. Nat. Genet. 23 (4), 452–456.

Meier-Kolthoff, J.P., Auch, A.F., Klenk, H.-P., Göker, M., 2013. Genome sequence-based species delimitation with confidence intervals and improved distance functions. BMC Bioinform. 14, 60.

Meier-Kolthoff, J.P., Göker, M., 2019. TYGS is an automated high-throughput platform for state-of-the-art genome-based taxonomy. Nat. Commun. 10 (1), 2182.

Meier-Kolthoff, J.P., Sardà Carbasse, J., Peinado-Olarte, R.L., Göker, M., 2022. TYGS and LPSN: a database tandem for fast and reliable genome-based classification and nomenclature of prokaryotes. Nucleic Acids Res. 50, D801–D807.

Meng, Q., Jiang, H., Hao, J.J., 2016. Effects of Bacillus velezensis strain BAC03 in promoting plant growth. Biol. Control 98, 18–26.

Montso, P.K., Alayande, K.A., 2024. Emerging Reservoir of Ecofriendly Resources within a Natural Endowment: Industrial Application of Bacterial and Fungal Endophytes. In: Microbial Essentialism. Elsevier.

Morelli, M., Bahar, O., Papadopoulou, K.K., Hopkins, D.L., Obradović, A., 2020. Role of Endophytes in Plant Health and Defense against Pathogens. Frontiers Media SA.

Ndlovu, B., Klaasen, J., Hughes, G., Fisher, F., 2024. An ethnobotanical survey investigating medicinal plants used by cape bush doctors to treat dermatophyte infections. Scientific African e02156.

Ni, J., Yu, L., Li, F., Li, Y., Zhang, M., Deng, Y., Liu, X., 2023. Macrolactin R from Bacillus siamensis and its antifungal activity against Botrytis cinerea. World J. Microbiol. Biotechnol. 39 (5), 117.
Olson, R.D., Assaf, R., Brettin, T., Conrad, N., Cucinell, C., Davis, J.J., Dempsey, D.M., Dickerman, A., Dietrich, E.M., Kenyon, R.W., Kuscuoglu, M., Lefkowitz, E.J., Lu, J., Machi, D., Macken, C., Mao, C., Niewiadomska, A., Nguyen, M., Olsen, G.J., Overbeek, J.C., Parrello, B., Parrello, V., Porter, J.S., Pusch, G.D., Shukla, M., Singh, I., Stewart, L., Tan, G., Thomas, C., VanOeffelen, M., Vonstein, V., Wallace, Z. S., Warren, A.S., Wattam, A.R., Xia, F., Yoo, H., Zhang, Y., Zmasek, C.M., Scheuermann, R.H., Stevens, R.L., 2022. Introducing the bacterial and viral bioinformatics resource center (BV-BRC): a resource combining PATRIC, IRD and ViPR. Nucleic Acids Res. gkac1003.
Ondov, B.D., Treangen, T.J., Melsted, P., et al., 2016. Mash: fast genome and metagenome distance estimation using MinHash. Genome Biol. 17, 1–14.
Overbeek, R., Olson, R., Pusch, G.D., Olsen, G.J., Davis, J.J., Disz, T., Edwards, R.A., Gerdes, S., Parrello, B., Shukla, M., Vonstein, V., Wattam, A.R., Xia, F., Stevens, R., 2014. The SEED and the rapid annotation of microbial genomes using subsystems technology (RAST). Nucleic Acids Res. 42, 206–214.
Petkau, A., Stuart-Edwards, M., Stothard, P., Van Domselaar, G., 2010. Interactive microbial genome visualization with GView. Bioinformatics 26, 3125–3126.
Prjibelski, A., Antipov, D., Meleshko, D., Lapidus, A., Korobeynikov, A., 2020 Jun. Using SPAdes De Novo Assembler. Curr. Protoc. Bioinformatics 70 (1), e102.
Qadri, M., 2022. Polyketides: bioactive secondary metabolites, biosynthesis, and their modulation. In: Endophyte Biology. Apple Academic Press, pp. 127–147.
Rabbee, M.F., Ali, M.S., Choi, J., Hwang, B.S., Jeong, S.C., Baek, K.-H., 2019. Bacillus velezensis: a valuable member of bioactive molecules within plant microbiomes. Molecules 24, 1046.
Rahman, F.B., Sarkar, B., Moni, R., Rahman, M.S., 2021. Molecular genetics of surfactin and its effects on different sub-populations of *Bacillus subtilis*. Biotechnol. Reports 32, e00686.
Ranjan, A., Rajput, V.D., Prazdnova, E.V., Gurnani, M., Bhardwaj, P., Sharma, S., Sushkova, S., Mandzhieva, S.S., Minkina, T., Sudan, J., Zargar, S.M., 2023. Nature's antimicrobial arsenal: non-ribosomal peptides from PGPB for plant pathogen biocontrol. Fermentation 9 (7), 597.
Robbins, T., Liu, Y.C., Cane, D.E., Khosla, C., 2016. Structure and mechanism of assembly line polyketide synthases. Curr. Opin. Struct. Biol. 41, 10–18.
Rodriguez-R, L.M., Gunturu, S., Harvey, W.T., Rosselló-Mora, R., Tiedje, J.M., Cole, J.R., Konstantinidis, K.T., 2018. The microbial genomes atlas (MiGA) webserver: taxonomic and gene diversity analysis of Archaea and Bacteria at the whole genome level. Nucleic Acids Res. 46 (W1), W282–W288.
Schappe, T., Ritchie, D.F., Thiessen, L.D., 2020. First report of Serratia marcescens causing a leaf spot disease on industrial hemp (Cannabis sativa). Plant Dis. 104 (4), 1248.
Sikora, E.J., Bruton, B.D., Wayadande, A.C., Fletcher, J., 2012. First report of the cucurbit yellow vine disease caused by Serratia marcescens in watermelon and yellow squash in Alabama. Plant Dis. 96 (5), 761.
Stamatakis, A., 2014. RAxML version 8: a tool for phylogenetic analysis and post-analysis of large phylogenies. Bioinformatics 30 (9), 1312–1313.
Subedi, N., Taylor, C.G., Paul, P.A., Miller, S.A., 2020. Combining partial host resistance with bacterial biocontrol agents improves outcomes for tomatoes infected with Ralstonia pseudosolanacearum. Crop Prot. 135, 104776.
Truyens, S., Weyens, N., Cuypers, A., Vangronsveld, J., 2015. Bacterial seed endophytes: genera, vertical transmission and interaction with plants. Environ. Microbiol. Rep. 7, 40–50.
Tsipinana, S., Husseiny, S., Alayande, K.A., Raslan, M., Amoo, S., Adeleke, R., 2023. Contribution of endophytes towards improving plant bioactive metabolites: a rescue option against red-taping of medicinal plants. Front. Plant Sci. 14, 1248319.
Viel, J.H., Kuipers, O.P., 2022. Modular use of the uniquely small ring a of mersacidin generates the smallest ribosomally produced lanthipeptide. ACS Synth. Biol. 11 (9), 3078–3087.
Wang, I.N., Smith, D.L., Young, R., 2000. Holins: the protein clocks of bacteriophage infections. Ann. Rev. Microbiol. 54 (1), 799–825.
Wang, X.Q., Bi, T., Li, X.D., Zhang, L.Q., Lu, S.E., 2015. First report of corn whorl rot caused by Serratia marcescens in China. J. Phytopathol. 163 (11−12), 1059–1063.
Ye, M., Tang, X., Yang, R., Zhang, H., Li, F., Tao, F., Li, F., Wang, Z., 2018. Characteristics and application of a novel species of Bacillus: Bacillus velezensis. ACS Chem. Biol. 13, 500–505.
Yin, Y., Wang, X., Zhang, P., Wang, P., Wen, J., 2024. Strategies for improving fengycin production: a review. Microb. Cell Factories 23 (1), 144.
Zakaria, L., 2023. Fusarium species associated with diseases of major tropical fruit crops. Horticulturae 9 (3), 322.
Zhang, K., Kries, H., 2023. Biomimetic engineering of nonribosomal peptide synthesis. Biochem. Soc. Trans. 51 (4), 1521–1532.
Zhang, L., Jin, M., Shi, X., Jin, L., Hou, X., Yu, Y., Liu, B., Cao, J., Quan, C., 2022. Macrolactin metabolite production by Bacillus sp. ZJ318 isolated from marine sediment. Appl. Biochem. Biotechnol. 194 (6), 2581–2593.
Zotchev, S.B., 2024. Unlocking the potential of bacterial endophytes from medicinal plants for drug discovery. In: Microbial Biotechnology.